optica

Release-free silicon-on-insulator cavity optomechanics: supplementary material

CHRISTOPHER J. SARABALIS*, YANNI D. DAHMANI, RISHI N. PATEL, JEFF T. HILL, AND AMIR H. SAFAVI-NAEINI*

Department of Applied Physics, and Ginzton Laboratory, Stanford University, Stanford, California 94305, USA

**Corresponding authors: sicamor@stanford.edu, safavi@stanford.edu*

Published 18 September 2017

This document provides supplementary information to "Release-free silicon-on-insulator cavity optomechanics," https://doi.org/10.1364/optica.4.001147. We present further details on simulating, modeling, and measuring the optical resonances of a fin cavity. We discuss how the grating coupler efficiency is determined from reflection spectra, an important parameter in determining the intracavity photon number and thereby the optomechanical coupling rates. We investigate the radiative limits of unreleased SOI fin resonators and present simulations and design a fin mechanical resonator with a radiation-limited quality factor of $Q = 120 \times 10^3$, exceeding material limits at room temperature. Finally, we numerically investigate a method for optically coupling to the "phase-protected", high Q modes of this structure, thus outlining an approach toward high Q, unreleased SOI optomechanical cavities.

https://doi.org/10.6084/m9.figshare.5331742

1. SIMULATIONS OF OPTICAL COUPLING AND LOSS RATES

By numerically solving for the optical resonances of the cavity, we quantify coupling rates to input-output and loss channels for various design parameters. FEM solutions to Maxwell's equations in the frequency domain are found for the cavity using COMSOL [1]. The optical eigenmodes are perturbatively coupled to radiative modes of free space and the coupling waveguides by a perfectly matched layer. By energy conservation, energy in the cavity $\mathcal{E}$ radiates away at a total rate κ_t such that $\mathcal{E}(t) = \mathcal{E}(0)e^{-\kappa_t t}$. This energy decay rate is related to the eigenvalue of the numerical solution λ as $\kappa_t = 2\mathrm{Im}\lambda$. The energy within and power $\mathcal{P}$ through the surfaces of a Gaussian pillbox around the cavity, shown in Figure S1, are related to the coupling rates κ_n as

$$\kappa = \sum_n \kappa_n = \sum_n \frac{\mathcal{P}_n}{\mathcal{E}}. \tag{S1}$$

The cavity described in this paper is coupled symmetrically on either side to waveguides that support TE and TM modes. We approximate the power in the TE and TM modes by integrating separately the $\mathbf{S}_{\mathrm{TE}} = -\mathbf{E}_x \times \mathbf{H}_z$ and $\mathbf{S}_{\mathrm{TM}} = \mathbf{E}_z \times \mathbf{H}_x$ polarizations of the Poynting vector over the surfaces normal to the axis of the waveguide (the z-axis in the figure). Additionally we compute the rate of radiation into free space modes $\kappa_\perp$ by integrating the power through the curved surface of the cylinder.

The coupling and loss rates as computed by the method described above informed a number of design decisions. In a cavity with reflection symmetry (reflection across the y-z plane in Figure S1), all electric fields of resonances of the cavity are either symmetric ("TM") or antisymmetric ("TE") and radiate exclusively into modes with the corresponding symmetry. TE resonances have zero coupling to TM modes of the waveguide. The cavity studied in this work intentionally breaks this reflection symmetry in order to break the mechanical degeneracy of the curved fin resonators. This symmetry breaking induces coupling of the now quasi-TE mode to the the TM mode of the waveguide, the rate of which is computed as described above. As the TM mode of the waveguide is dropped by the TE grating coupler, TM coupling is regarded as a loss channel.

The defect of the cavity described in this paper is a reduction in the width of the fins. Decreasing the length over which the fin's width is varied increases the coupling to free space modes. A competing effect is that smaller mode volumes result in higher optomechanical coupling rates. We choose the length of the parabolic fin width defect such that the free space radiative losses are comparable to scattering into the TM mode $\kappa_\perp \approx \kappa_{\mathrm{TM}}$ for the TE_{00} optical resonance. Making the cavity longer reduces the rate of radiation into free space without affecting the fundamental Q-limiting, symmetry-breaking induced radiation into the dropped TM waveguide modes.

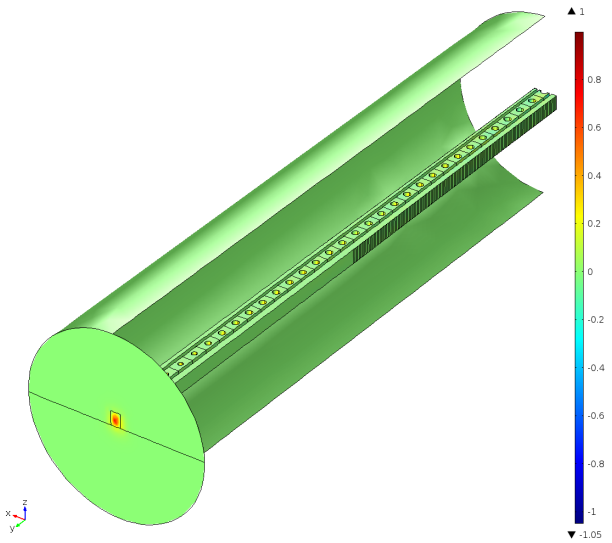

Fig. S1. The energy in and power through the Gaussian pillbox shown, cutaway to expose the cavity for clarity, is used to compute the optical coupling rates to various input-output and loss channels. Here color indicates the normalized power through the surface for the TE_{00} mode, dominated by coupling to the TE mode of the waveguide. The coupling waveguide and simulation domain extends beyond the pillbox and has a cylindrical perfectly matched layer.

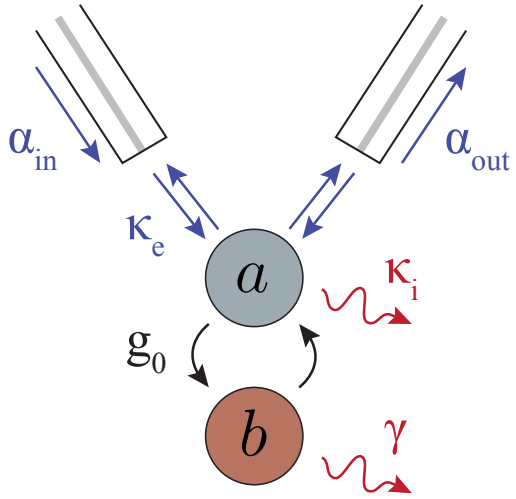

Fig. S2. Optical coupling scheme. The optical cavity represented by the annihilation operator a is coupled to a fiber on either side for transmission and reflection measurements enabling independent determination of intrinsic κ_i and extrinsic κ_e coupling rates. Coupling to the mechanical mode b is also diagrammed and discussed in the main text.

2. INPUT-OUTPUT THEORY FOR OPTICAL MODES OF THE CAVITY

In this section of the SI, we describe the double-sided optical coupling scheme and relate the transmission and reflection spectra to the efficiency of the grating coupler η_{gc} and the intrinsic and extrinsic damping rates κ_i and κ_e. The resulting model allows us to relate the power incident on the cavity to the intracavity photon number α^2, a quantity necessary for extracting the optomechanical coupling rate g_0.

We can use the *input-output relations* to find an equation of motion for the cavity operator a and relate it to the light incident on a_{in} and leaving from a_{out} the cavity [2]. In a frame rotating at the laser drive frequency ω_L

$$\dot{a} = i\Delta a - \frac{\kappa_t}{2} + \sqrt{\kappa_e}a_{in} \tag{S2}$$

where $\kappa_t = \kappa_i + 2\kappa_e$ and $\Delta = \omega_L - \omega_c$. The factor of 2 for κ_e results from the double-sided coupling of the cavity. Here we've set the input operator for the output fiber to zero. The steady state $\dot{a} = 0$ solution for the cavity operator is simply

$$a = -\frac{\sqrt{\kappa_e}}{i\Delta - \frac{\kappa_t}{2}}a_{in}. \tag{S3}$$

Since for transmission the output operator is related to the cavity operator as $a_{out} = \sqrt{\kappa_e}a$, the steady state output is

$$a_{out} = -\frac{\kappa_e}{i\Delta - \frac{\kappa_t}{2}}a_{in} \tag{S4}$$

which when driven coherently $a \to \alpha$, and after adding the input and output grating coupler efficiencies, yields the transmission spectrum

$$T = \left|\frac{\alpha_{out}}{\alpha_{in}}\right|^2 = \eta_{gc}^2\frac{\kappa_e^2}{\Delta^2 + \frac{\kappa_t^2}{4}}. \tag{S5}$$

We assume that the input and output grating couplers have equal efficiencies. Similarly the intracavity photon number is

$$\alpha^2 = \eta_{gc}\frac{\kappa_e}{\Delta^2 + \frac{\kappa_t^2}{4}}\alpha_{in}^2. \tag{S6}$$

By fitting a Lorentzian to the transmission about a resonance we can determine $\eta_{gc}^2\kappa_e$ and κ_t. We need an independent way of determining the grating coupler efficiency and so look to the reflection spectrum described in Section 3.

3. OPTICAL CHARACTERIZATION OF THE GRATING COUPLER EFFICIENCIES

From the reflection spectrum we can infer how the grating coupler efficiency η_{gc} varies over the scan range. The reflection spectrum contains the interference of two reflection paths of roughly equal intensity : reflections off the end facet of the cleaved fiber and light reflected off the cavity. The former is a nearly constant 3% over the scan range. The amplitude reflection coefficient is readily measured by lifting the fiber from the grating coupler. The latter reflection is transmitted through the grating coupler and then bounces off the cavity – the cavity acts as a mirror off resonance – before being scattered by the grating coupler into the fiber. The reflected optical amplitude is

$$\alpha_{out} = \left(r_1 + \eta_{gc}e^{i2k\sum nL}\right)\alpha_{in}. \tag{S7}$$

The factor of η_{gc} appears as the input and output amplitude transmission coefficient of the grating coupler are equal by reciprocity and their square is the power tranmission coefficient. The resulting reflection spectrum contains slowly and quickly varying contributions each of which can be used with knowl-

edge of r_1 to determine η_{gc}.

$$\left|\frac{\alpha_{out}}{\alpha_{in}}\right|^2 = \underbrace{|r_1|^2 + |\eta_{gc}|^2}_{\text{slowly varying}} + \underbrace{2\,|r_1\eta_{gc}|\cos\left(2k\sum nL\right)}_{\text{quickly varying}} \quad \textbf{(S8)}$$

A simple linear error propagation shows $\delta\eta_{slow} = -2r_1\delta r \approx -0.36\delta r$ and $\delta\eta_{fast} = -\frac{\eta_{gc}}{r_1}\delta r \approx -0.94\delta r$.

From our measurements, we estimate the uncertainty for the input coupling efficiency: $\eta + \delta\eta$. In particular, we find that $\delta\eta/\eta \approx 5\%$. This is the primary source of uncertainty in our determination of g_0. Our fit to the measured spectrum determine $g_0|\alpha| \propto \sqrt{\eta}g_0\sqrt{P_{in}}$. As such, the uncertainty in η causes an uncertainty in g_0 as $\delta g_0/g_0 = \delta\eta/2\eta$. We find that $\delta\eta/\eta \approx 5\%$, so we have about 2.5% uncertainty in g_0.

To summarize, our calibration uses the interference between the reflection at the fiber facet, and the reflection of the light entering the system through the grating coupler and reflecting off the end of the photonic crystal to obtain an accurate estimate of the grating couplign efficiency η. Errors in this estimate of η (on the order of 5%) are propagated to the determination of g_0.

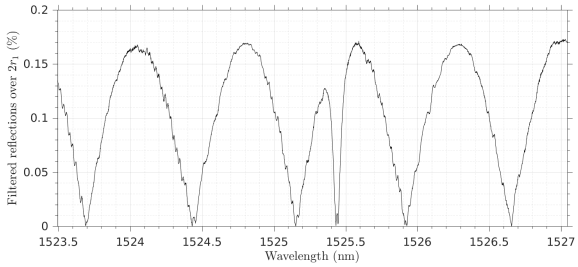

Fig. S3. The interference between reflections from the fiber facet and off the cavity give rise to the beat signal filtered out above from the reflection spectrum. The absolute value divided by $2r_1$ is plotted; the peaks are the power efficiency of the input grating coupler.

4. A HIGH Q FIN RESONATOR

The Γ-point mechanical modes of fins are used in the design of the cavities measured here because they are easy to couple to optical standing waves (as described in Section 5). These modes radiate into surface and bulk acoustic waves resulting in Q's of ~ 100. While this makes these cavities already competitive with microwave components on SOI, many applications call for mechanical resonators with higher quality factors and optomechanical cavities with high cooperativities, motivating the use of the higher K states in the phase-protected, radiation-free region of the fin dispersion [3].

For a Γ-point resonator, a simple curved fin gives finer control over the mode's size and shape, enabling appreciable optomechanical coupling. A ring resonator design, made by looping a fin is a simple way to confine high K mechanical modes. Since our principle motivation is to build an optomechanical cavity which benefits from small mode volumes [1], we take a different approach similar to the design of a photonic crystal cavity. By modulating the width of a fin, we can open a bandgap in the mechanical dispersion and make a phononic crystal Bragg mirror. Two of these mirrors can be used to make a linear Fabry-Pérot cavity, as shown in Figure S4a, which can replace the curved fins of the measured device.

Our goal is to design a high K resonator with radiation-limited Q's exceeding typical room temperature material limits of $\sim$ 10k. For ease of integration into a cavity we choose a unit cell of a fin with single-sided sinusoidal width variations. This structure contains two modes of interest: excitations of the thinner and excitations of the thicker regions of the fin plotted in Figure S4b. When designing a crystal cavity, it is helpful to know how the frequencies of relevant modes change with the modulation parameter, here the peak-to-peak width variation of the fin. From this we choose a defect cell with 15 nm width variation which is varied quadratically to 30 nm in the mirror region. This choice of defect and mirror parameters avoids mixing between the two bands. From the difference in frequency between mirror and defect region and a characteristic velocity we can estimate the length scale over which the bound state decays. Using $v_{saw} = 3300\ \frac{m}{s}$ we have a decay length of approximately 9 μm. For $a = 227$ nm, this is 40 periods.

The resonator in Figure S4d oscillates at 5.7 GHz and has a Q of 120×10^3. It's 80 unit cells long with the quadratic defect spanning 30 unit cells. By using mechanical modes with wavenumber $\nu = 2.2\ \mu m^{-1}$ we were able to cull radiation and increase the Q by three orders of magnitude relative to the Γ-point resonator. As with photonic crystal cavities, there are still design-dependent radiative losses despite the existence of bound, radiation-free 1D waveguide modes of the unit cell which are decreased by making the resonator longer with a more slowly varying defect. With a design for a high K, high Q fin resonator, we turn our attention to coupling these modes to the optics.

5. COUPLING OPTICS TO A HIGH Q FIN RESONATOR

Our focus on Γ-point mechanical modes greatly simplifies coupling to optical modes easy. As the optomechanical coupling

$$g_0 = -\frac{\omega}{2}\frac{\langle \mathbf{E}|\delta_{\mathbf{u}}\varepsilon\cdot\mathbf{u}|\mathbf{E}\rangle}{\langle \mathbf{E}|\varepsilon|\mathbf{E}\rangle}$$

is first order in the mechanics $\mathbf{u}$ but scales as the optical intensity $|\mathbf{E}|^2$, phase variations of the mechanical field along the propagation direction can diminish or completely cancel the coupling rate. More simply, if we take a snap-shot of the motion, regions of the fin bent toward the cavity lower its frequency, cancelled by the adjacent half-wavelength moving away from the cavity. This makes coupling mechanical modes with nonzero wavenumber to optical standing waves difficult motivating the use of the Γ-point modes for the cavities investigated here. One way of circumventing this effect in high confinement cavities is to engineer the optical and mechanical modes envelopes such that envelope modulation leads to large coupling. For example given modes confined over a handful of lattice periods, a fundamental optical mode with Gaussian envelope and first excited mechanical mode with a node at the cavity's center can have coupling rates dominated by the unit cell where the envelopes intersect. We present a more general strategy for which *a unit cell*, independent of the envelopes, of an optomechanical crystal exhibits appreciable coupling to high K modes, in particular those of the fin resonator described above. To verify the coupling rate of this "2k" design, the Bloch functions of the unit cell for the optics and mechanics are used to compute unit cell coupling rates g_Δ and estimate cavity coupling rates g_0.

We adopt an analytical approach for computing g_0 from Safavi-Naeini *et al.*, aspects of which we repeat here with slight

[1] Cooperativity C scales as L^{-1} for a cavity of length L.

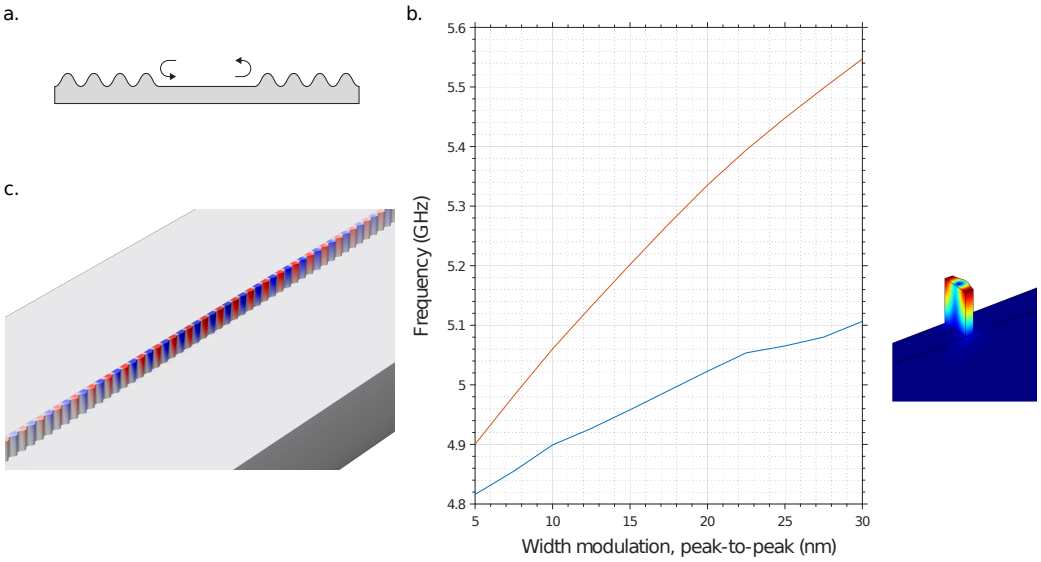

Fig. S4. a. Phononic crystal mirrors made by modulating the width of a fin can be used to make a high Q, release-free mechanical Fabry-Pérot. **b.** The unit cell of these mirrors is a fin with single-sided sinusoidal width modulations. Here the fin is 63 nm from the flat to the troughs of the opposing sinusoid and the period $a = 227$ nm is chosen such that the X-point modes with wavenumber $\nu = 2.2\ \mu\text{m}^{-1}$ are radiation free. The width modulation opens up a bandgap at the X-point which varies with the peak-to-peak width modulations as shown here. **c.** These modes are the basis of the 80 unit cell long resonator shown which has a quadratic defect over 30 unit cells for which the width variations are swept from 15 to 30 nm peak-to-peak resulting in a Q of 120k.

modifications [4]. If we factorize the optical

$$\mathbf{E}(x,y,z) = f_o(z)\,\tilde{\mathbf{e}}(x,y,z)$$

and mechanical mode

$$\mathbf{u}(x,y,z) = f_m(z)\,\tilde{\mathbf{u}}(x,y,z)$$

where the Bloch functions $\tilde{\mathbf{e}}$ and $\tilde{\mathbf{u}}$ are periodic in z with period a, we can rewrite the optomechanical interaction rate g_0 in terms of the envelopes f_0 and f_m

$$g_0 = g_\Delta \frac{\int \mathrm{d}z f_o^2(z) f_m(z)}{\int \mathrm{d}z f_o^2(z) \sqrt{\int \mathrm{d}z f_m^2(z)}}.$$

The unit cell coupling rate g_Δ is defined in terms of the Bloch functions as

$$g_\Delta = -\frac{\omega}{2}\frac{\langle\tilde{\mathbf{e}}|\delta_{\mathbf{u}}\varepsilon\tilde{\mathbf{u}}|\tilde{\mathbf{e}}\rangle}{\langle\tilde{\mathbf{e}}|\varepsilon|\tilde{\mathbf{e}}\rangle}\sqrt{a}$$

and has units of $\text{Hz}\cdot\sqrt{\text{m}} = \text{kHz}\cdot\sqrt{\mu\text{m}}$. Assuming Gaussian envelopes, we can use g_Δ to calculate g_0 for a full cavity.

The design we propose is, as with the fin cavities measured, a nanobeam with adjacent fins. The nanobeam has a period of twice the fin's modulation $a = 454$ nm. It's 240 nm wide. The holes are elliptical with a minor axis of 140 nm transverse to the direction of propagation and a major axis of 200 nm. The fins are spaced from the nanobeam by 60 nm. For this study, the fin has a width modulation that is 30 nm peak-to-peak.

The modes of this structure are shown in Figure S5. The optical mode is the first excited TM mode, with an electric field that is symmetric with respect to reflections about the symmetry plane. The mechanical mode, corresponding to the red curve in Figure S4, exhibits higher coupling rates than its lower frequency counterpart. For this $2k$ design, the wavevector of the mechanics is twice that of the optics. Radiation pressure forces go as $|\mathbf{E}|^2$

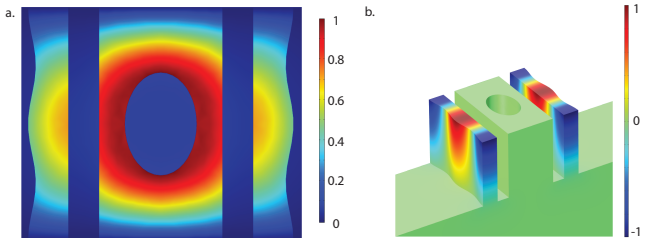

Fig. S5. This $2k$ unit cell has 5.5 GHz mechanical modes in **b.** with twice the wavenumber as the optical mode in **a.**. The out-of-plane component of the electric displacement field is plotted for the 191 THz optical X-point mode. The transverse component of the mechanical displacement is plotted.

resulting in two spatial phase factors, one that's constant and one that goes as e^{i2kz}. The latter component drives the mechanical modes shown in Figure S5b achieving unit cell coupling rates g_Δ of $2\pi \times 106\ \text{kHz}\sqrt{\mu\text{m}}$. The optimal cavity coupling rate is

$$g_0 = \frac{1}{(4\pi)^{\frac{1}{4}}}\frac{g_\Delta}{\sqrt{L}}$$

where L is the standard deviation of the mechanical envelope [4]. Taking L to be 30 periods give us $g_0/2\pi = 22$ kHz. The obtained cooperativity, $C = 4g_0^2/\kappa\Gamma$ for mechanical and optical linewidth Γ and κ, of this cavity compared to that of the Γ-point design for the TE_{00}, f_0 mode pair shows that this design can allow access to the large cooperativity regime important in quantum optomechanics.

In conclusion, we find that systematically extending the cavity design presented experimentally in this work, we can gain access to cavity modes with lowloss and optomechanical resonance in unreleased silicon-on-insulator.

REFERENCES

1. "COMSOL Multiphysics v5.0," .
2. C. Gardiner and M. Collett, "Input and output in damped quantum systems: Quantum stochastic differential equations and the master equation," Physical Review A **31**, 3761 (1985).
3. C. J. Sarabalis, J. T. Hill, and A. H. Safavi-Naeini, "Guided acoustic and optical waves in silicon-on-insulator for brillouin scattering and optomechanics," APL Photonics **1**, 071301 (2016).
4. A. H. Safavi-Naeini and O. Painter, "Design of optomechanical cavities and waveguides on a simultaneous bandgap phononic-photonic crystal slab," Optics express **18**, 14926–14943 (2010).